50 nm Thick AlN Resonant Micro-Cantilever for Gas Sensing Application

P. Ivaldi, J. Abergel, G. Arndt, P. Robert, P. Andreucci, H. Blanc, S. Hentz, E. Defay
CEA/LETI-MINATEC
Grenoble, France
Email: paul.ivaldi@cea.fr

***Abstract*— We present the fabrication and characterization of a $90\mu\mathrm{m} \times 40\mu\mathrm{m} \times 885\mathrm{nm}$ piezoelectric micro-cantilever resonator containing a 50nm thick Aluminum Nitride (AlN) piezoelectric film for transduction. Material characterizations demonstrate that our AlN deposition technique enables the fabrication of ultra-thin films with high piezoelectric coefficient $e_{31} = 0.78\mathrm{C.m}^{-2}$. Fully electrical actuation and detection of the cantilever resonance behavior is evidenced using on-chip electric bridge and instrumented probe trans-impedance amplifier. Finally, based on Allan deviation measurement results, we demonstrate the potential of this cantilever for gas detection with an expected limit of detection equal to $70\mathrm{zg}.\mu\mathrm{m}^{-2}$**

I. Introduction

Miniature and battery powered electronic noses are emerging as an inexpensive and powerful tool for a wide range of applications from security and defense [1] to health care [2]. One critical issue in the design of such gas sensor system concerns the choice of the sensing element which must demonstrate high level of integrability, reliability, resolution and low power functioning. For this matter, gravimetric sensors based on Nano/Micro Electromechanical Systems (N/MEMS) such as FBAR [3], SAW [4], CMUT [5], Contour mode resonator [6], and flexural resonators [7] have attracted considerable interests. Along the past twenty years, out standing performances have been evidenced, with a typical limit of detection ranging from the part per cent down to the part per billion.

In the meantime, piezoelectric thin film technology has been the focus of extensive research efforts. With the very recent demonstration of few micrometers long and hundreds of nanometers thick piezoelectric beam actuators [8], [9] piezoelectric transduction is now witnessing an increased interest in the NEMS community. Piezoelectricity is particularly interesting compared to more classical NEMS transduction techniques like thermo-elastic, capacitive or magnetomotive actuation and optical, piezoresitive, electrostatic and inductive detection. Especially, it enables high power efficiency [10] and fully integrated transduction [11]. Among possible piezoelectric materials, AlN provides several advantages, such as high piezoelectric coupling, low dielectric loss, good mechanical properties and compatibility with CMOS processing. However, from the technological point of view, AlN piezoelectric NEMS still represent a real challenge and the fabrication of tenth of nanometers thick AlN films that retain superior material properties has become a key issue.

Combining the aforementioned advantages with the high gravimetric performances of NEMS resonators, piezoelectric NEMS could represent a very interesting paradigm for portable gas sensor systems. It is thus of great importance to investigate in detail their gas sensing performances. Until now, micro scale piezoelectric (PZE) flexural beam resonators have been demonstrated as gravimetric sensor for mass [11], [12] biological [13] and gas [10] sensing applications but scaling rules haven't been analyzed yet.

As a step towards the demonstration of AlN piezoelectric NEMS, we report the fabrication and full electrical characterization of a $90\mu\mathrm{m} \times 40\mu\mathrm{m} \times 885\mathrm{nm}$ micro-cantilever actuated and detected by means of a 50nm thick AlN piezoelectric layer. We demonstrate that our AlN deposition technique enables high piezoelectric e_{31} coefficient up to $0.78\mathrm{C.m}^{-}2$ for film thicknesses between 50nm and 800nm. In order to anticipate the extremely low signal to background ratios of PZE NEMS, the electrical characterization is performed using an on-chip electrical bridge and a dedicated trans-impedance amplifier electronic circuit directly mounted on the tester probes. Signal reduction via parasitic capacitance is thus avoided and both signal over background and signal over noise ratios are improved. Finally, the Allan deviation of the whole measurement set-up is assessed in order to calculate the expected limit of detection for gas sensing applications.

II. Device Fabrication

A. 50nm thick AlN films characterization

As discussed in the introduction, the fabrication of tenth of nanometer thick AlN films with sufficiently high piezoelectric properties and low residual stress to be implemented for N/MEMS transduction, is a great technological challenge itself. Thus, before the fabrication of any devices, it is of great importance to characterize the AlN films properties enabled by our DC reactive magnetron sputtering deposition process. To do so, Pt(100nm)/ AlN / Pt (100nm) stacks are deposited on 8 inches silicon substrates with AlN thickness and deposition DC bias varied from 50nm to 800nm and from 10W to 80 W, respectively. The residual stress of the different layers is assessed by measuring the radius of curvature of the processed wafers before and after the deposition of each layer. Fig 1 (a) evidences the strong dependency of the AlN stress on both the

978-1-4244-6400-5/10/$26.00 ©2010 IEEE

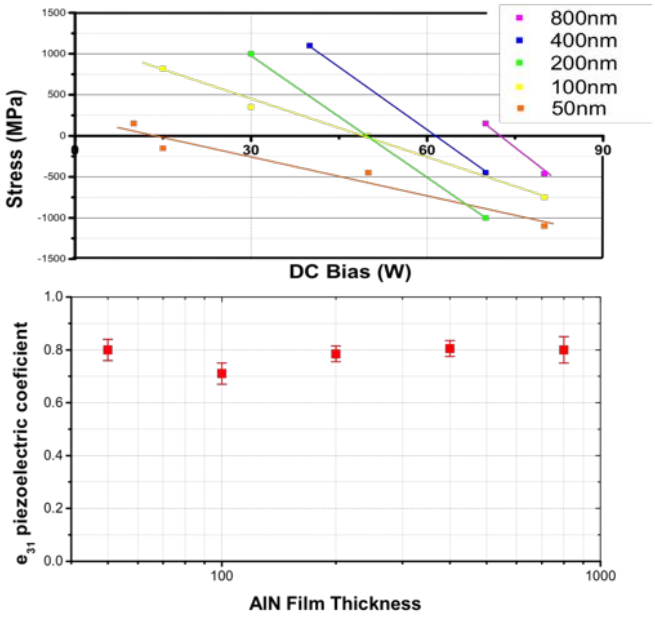

Fig. 1. Top graph: Stress in the AlN layer as a function of the DC bias power used for deposition and nominal thickness. Bottom graph variation of the e_{31} piezoelectric coeficient with AlN film thickness

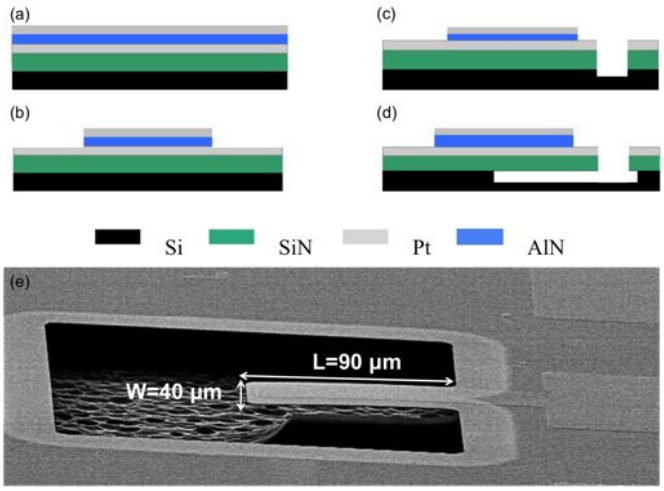

Fig. 2. (a) Deposition of the full material stack Si_3N_4 (structural)/ Pt (bottom) / AlN (active) / Pt (top). (b) First lithographic step, Argon plasma IBE patterning of top Pt and AlN active layer. (c) Second lithographic step, Argon plasma patterning of the bottom Pt electrode, RIE of the Si_3N_4 structural layer. (d) XeF_2 plasma isotropic etch of Si substrates for structure release. (e) SEM image of the fabricated Micro-cantilever

thickness and the deposition DC bias. Depending on the case, tensile or compressive values are obtained. The crystallinity of the AlN films is also characterized by XRD technique. All fabricated films are fully c-axis oriented with rocking curve Full Width at Half Maximum (FWHM) increasing with decreasing thickness. However a satisfying value of 2.40 is obtained for the 50nm thick layers. Finally, capacitive structures are fabricated by patterning the top Platinum electrode in order to use the method described in [14] for e_{31} piezoelectric coefficient measurement. Experimental results show that the e_{31} piezoelectric coefficient retains a high value of $0.78\mathrm{C.m}^2$ for all tested AlN film thicknesses. Up to our knowledge, it is the highest value ever reported in the literature for 50nm thick AlN films.

B. Micro-cantilever fabrication

The fabrication of the cantilever starts with the deposition of a stack Si_3N_4 (structural)/ Pt (bottom) / AlN (active) / Pt (top) over an 8 inches Silicon wafer. Special attention is given to tailor the residual stress of each layer in order to avoid static bending of released structures. The $700nm$ thick Si_3N_4 structural layer is deposited by Low Pressure Chemical Vapor Deposition with $600\mathrm{MPa}$ tensile stress. The $50nm$ thick AlN layer is deposited using DC reactive magnetron sputtering with $150\mathrm{MPa}$ tensile stress. The bottom and top Pt electrodes are deposited by sputtering and their residual stress is tuned to $600\mathrm{MPa}$ by rapid thermal annealing.

A two UV-lithography steps process is then performed for the cantilever fabrication. The first step is used to pattern the top electrode and active AlN layers by Argon plasma Ion Beam Etching (IBE) and the second one to pattern the bottom electrode and structural layers by subsequent Argon plasma IBE and C_4F_2 Reactive Ion Etching (RIE). Finally, the release of the cantilevers is obtained with XeF_2 plasma isotropic etch of the Si substrate. Fig 2(e) gives an electronic microscope view of the fabricated cantilevers, with distinct AlN active / top Pt electrodes areas whereas the bottom Pt electrodes covers all the remaining surface.

III. Device Characterization

A. Equivalent Circuit

The working principle of PZE heterogeneous bi-morph is now well known [15]. When a potential difference is applied between the top and bottom electrode, the AlN active layer expands and gives rise to a bending moment. Reversely, when an external bending is imposed to the beam, the non null average strain in the AlN active layer produces an electric field which can be detected by measuring the amount of charges created on the surface of the electrodes. If the applied electric field is a sine wave at a frequency close to the n-th resonance frequency of the beam $\omega_n = \left(\frac{\alpha_n}{L}\right)^2 \sqrt{\frac{YI}{\rho A}}$, the electrical response of the cantilever can be modeled with a Buterworth Van Dyke (BVD) equivalent circuit (Fig 3 (b)). An analytical formula for each component of the circuit can be derived from the expression of the admittance given in [15]:

$$C_0 = \epsilon_{33}\frac{wl}{h_{AlN}} \quad ; \quad C_n = \frac{\mathrm{M_V}\left(\frac{\partial W_n}{\partial x}(l)\right)}{\rho A l \omega_n^2} \qquad (1)$$

$$L_n = \frac{1}{C_n\omega_n^2} \quad ; \quad R_n = \frac{Q_n}{\omega_n C_n} \qquad (2)$$

Here Y, I, ρ, A, w, l are the Young modulus, the quadratic momentum, the linear mass, the cross section area, the width

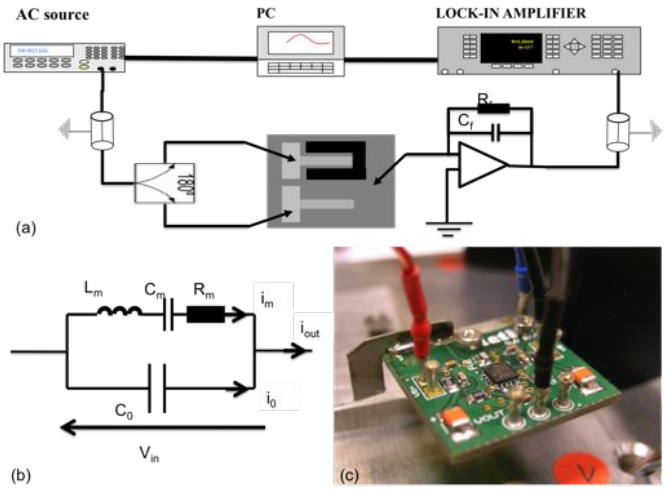

Fig. 3. (a) Experimental setup used for the electrical characterization, with on-chip half bridge and trans-impedance amplifier circuit directly mounted on the tester probes

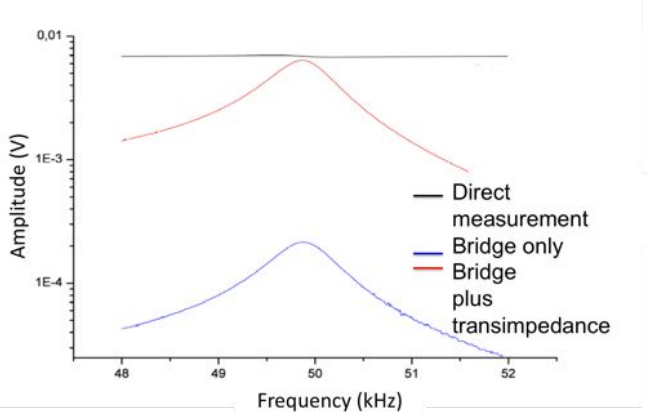

Fig. 4. Detection of the first resonance mode with and without the use of the bridge and of the trans-impedance amplifier

and length of the beam, respectively. ϵ_{33} is the dielectric constant of AlN, $\mathrm{M_V}$ is the piezoelectric moment, W_n and Q_n are the n-th mode shape and quality factor.

B. Feedthrough Capacitance cancellation and transimpedance amplification

Taking into account the typical value of the different components of the BVD model for our cantilever, the feedthrough capacitance C_0 introduces an unwanted signal which swamp the motional signal. Thus an electrical bridge [16] is required to compensate for this background signal. So, we take advantage of the presence of the bottom electrode on the majority of the chip area by using an on-chip unreleased cantilever as dummy capacitor (Fig3(a)). In this configuration, the output signal is limited by the different shunt capacitances arising from the cable and detector input. To overcome this difficulty, a trans-impedance amplifier circuit directly mounted on the tester probes is implemented. For the circuit design, the feedback resistor R_f and capacitor C_f value are set to $1\mathrm{M}\Omega$ and 1pF respectively in order to obtain a trans-impedance value of $0.5\mathrm{M}\Omega$ and a bandwidth of $1\mathrm{MHz}$. Because of its very low noise figure, the ADA4817 operational amplifier is chosen as active component. Theoretically, this trans-impedance amplifier circuit provides an increased the signal over noise ratio by a factor of 40 compared to classical non inverting voltage amplifier with equivalent bandwidth.

IV. Experimental results

A. Frequency behavior

The frequency response for the cantilever exhibits four resonance peaks at 88kHz, 535kHz, 1.25MHz and 3.4MHz (Fig 5) in good agreement with the analytical predictions 92kHz, 578kHz, 1.72MHz and 3.17MHz. Thanks to the bridge architecture, the background signal is reduced by two orders of magnitude but not canceled totally. Separate measurement of the static capacitance of the cantilever and dummy capacitor shows a $\pm 1\%$ mismatch compliant with the observed background signal level. The use of the trans-impedance amplifier is also proven to be beneficial with an increase of the signal over background ratio of a factor 4. More detailed characterizations are required to understand the difference between the experimental and theoretical improvement factor.

B. Allan deviation

We further investigate the characterization of our cantilever in order to evaluate its gas sensing performances. To be used as a chemical sensor, the cantilever should be covered by a so-called functionalization layer. When exposed to gaseous chemical species with affinity to the functionalization layer, the absorption induced increase of the vibrating mass will shift downwards the resonance frequency. Using a electronic feedback loop, typically a phase locked-loop, the frequency change can be tracked. Thus, the concentration variation of the chemical species can be monitored continuously. The performance of such sensor system are generally evaluated in terms of limit of detection, or smallest concentration variation, δm_{surf} expressed in $\mathrm{zg}.\mu\mathrm{m}^{-2}$ in order to be independent from chemical consideration. An analytical formula of this figure of merit can be obtained by mathematical differentiation of the resonance frequency formula under the assumption of a small accreted mass:

$$\delta m_{surf} = \frac{m_{tot}}{2WL}\frac{\delta\omega}{\omega_n} \tag{3}$$

where m_{tot} is the total mass of the beam. The term $\frac{\delta\omega}{\omega_n}$ is the frequency stability in the whole electrical loop or smallest measurable relative frequency variation. It depends on the total frequency noise and can be evaluated experimentally by measuring the the Allan deviation. Fig 6 presents the results of such experiment for our cantilever with a minimum value

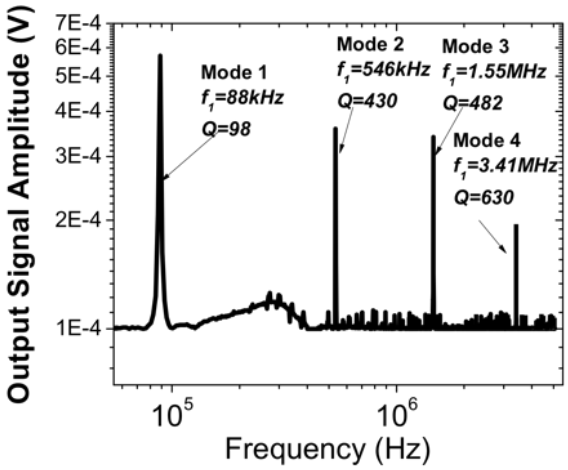

Fig. 5. Electrical frequency response

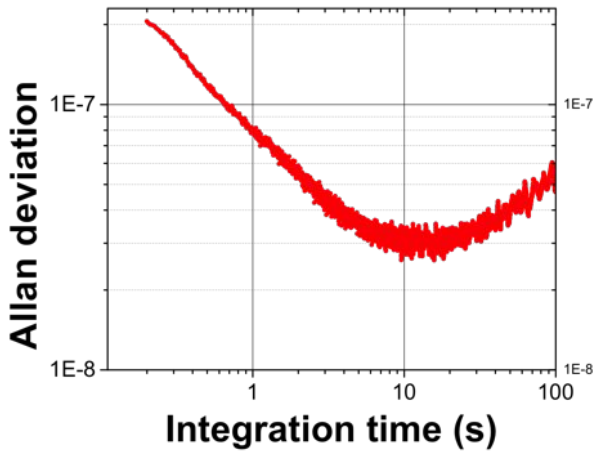

Fig. 6. Allan deviation in air for $V_in = 0.2V$

TABLE I
STATE OF THE ART OF GAS SENSING

device	resolution (in zg.μm^{-2})
BAW [3]	1000
SAW [4]	700
CMUT [5]	71
Flexural cantilever [7]	20

of 3×10^{-8} for 10 seconds integration time. Using (3), this corresponds to a limit of detection equal to $70zg.\mu m^{-2}$, which is one of the lowest value reported so far, as illustrated in table 1.

V. CONCLUSION

We have demonstrated that 50nm thick AlN films can retain sufficiently good piezoelectric properties to be implemented as a transducer in MEMS. We have also demonstrated the full electrical characterization of a $90\mu m \times 40\mu m \times 885nm nm$ cantilever using a very efficient detection scheme based on on-chip electrical bridge and instrumented probes trans-impedance amplifier. Finally, we have measured the the Allan deviation of the whole experimental setup and have used the result to calculate an expected limit of detection for gas sensing equals to $70zg.\mu m^{-2}$. This value is comparable to the best performances reported in the literature and lot of room still remains for further optimizations like increasing the driving voltage, reducing noise and using thinner Si_3N_4 films. Thus we conclude on the exceptional prospects given by this technology for high sensitivity gas detection.

ACKNOWLEDGMENT

The authors would like to thank Matt Matheny, G.Villaluonga, R. Karabalin and F. Feng for helpful discusions and corrections. We also kindly acknowledge the IFC Society for the student travel support

REFERENCES

[1] P. Lewis, et al., "Recent advancements in the gas-phase MicroChemLab," IEEE SENSORS JOURNAL, JUN 2006 2006.
[2] C. Di Natale, et al., "Lung cancer identification by the analysis of breath by means of an array of non-selective gas sensors," BIOSENSORS & BIOELECTRONICS, 2003.
[3] H. Zhang and E. Kim, "Micromachined acoustic resonant mass sensor," JOURNAL OF MICROELECTROMECHANICAL SYSTEMS, 2005
[4] W. Wang, et al., "High frequency stability oscillator for surface acoustic wave-based gas sensor," SMART MATERIALS & STRUCTURES, 2006
[5] H. J. Lee, et al., "CMUT as a chemical sensor for DMMP detection,"IEEE International Frequency Control Symposium, 2008
[6] C. Zuniga, et al., "Nanoenabled microelectromechanical sensor for volatile organic chemical detection," APPLIED PHYSICS LETTERS vol. 95 2009
[7] D. Lange, et al., "CMOS resonant beam gas sensing system with on-chip self excitation," MEMS 2001. 14th IEEE International Conference
[8] R. B. Karabalin, et al., "Piezoelectric nanoelectromechanical resonators based on aluminum nitride thin films," APPLIED PHYSICS LETTERS vol. 95, 2009.
[9] N. Sinha, "Piezoelectric aluminum Nitride nanoelectromechanical actuators," APPLIED PHYSICS LETTERS, vol. 95, 2009.
[10] J. D. Adams, et al., "Nanowatt chemical vapor detection with a self-sensing, piezoelectric microcantilever array," APPLIED PHYSICS LETTERS, vol. 83, 2003.
[11] S. Gonzalez-Castilla, et al., "Electrical detection of the mechanical resonances in AlN-actuated microbridges for mass sensing applications," APPLIED PHYSICS LETTERS, vol. 82 2008
[12] S. Shin, et al., "A multisized piezoelectric microcantilever biosensor array for the quantitative analysis of mass and surface stress," APPLIED PHYSICS LETTERS, vol. 87 2008
[13] Y. Lee, et al., "Piezoelectric micro cantilever sensor for non-labeling detection of biomarker," IEEE Sensors, 2008
[14] E. Defay, et al., "Modified free vibrating beam method for characterization of effective e(31) coefficient and leakage resistance of piezoelectric thin films," REVIEW OF SCIENTIFIC INSTRUMENTS, OCT 2006 2006.
[15] M. Brissaud, "Modelling of non-symmetric piezoelectric bimorphs," JOURNAL OF MICROMECHANICS AND MICROENGINEERING, vol. 14, 2004.
[16] J. E.-Y. Lee and A. A. Seshia, "Parasitic feedthrough cancellation techniques for enhanced electrical characterization of electrostatic microresonators," SENSORS AND ACTUATORS: A PHYSICAL, vol. 156, 2009